LINC-NIRVANA

The **L**BT **IN**terferometric **C**amera and **N**ear-**I**nfra**R**ed / **V**isible **A**daptive i**N**terferometer for **A**stronomy

A collaborative project of the MPIA Heidelberg, INAF-Arcetri, Universität zu Köln, and MPIfR Bonn

http://www.mpia.de/LINC

LINC-NIRVANA

-

GWS Alignment verification after shipping in Heidelberg report

Doc. No.	LN-INAFP-TN-AO-007
Short Title	GWS Verification Report HD
Issue	0.1
Date	28 March 2012

	Name	Date	Signature
Prepared	V. Viotto, M. Bergomi	28 March 2012	
Approved	N. Surname	dd month yyyy	
Released	N. Surname	dd month yyyy	

Change Record

Issue	Date	Sect.	Reason/Initiation/Documents/Remarks
0.1	28.03.2012	all	New document

Contents

List of Figures

List of Tables

This page is intentionally left blank

1 Scope

In this document the results of the verification tests of the Ground layer Wavefront Sensor DX (Unit 1) , performed in Heidelberg after the shipping from Padova, are described. These tests have been performed in March 2012.

2 Applicable documents

No.	Title	Number & Issue
AD1	Ground layer Wavefront Sensor Verification & Acceptance report	LN-INAFP-VER-AO-001 Issue 0.3
AD2	GWS error budget	LN-INAFP-DES-GEN-001 Issue 0.3

3 Terms and Abbreviations

LN	LINC-NIRVANA
FoV	Field of View
GWS	Ground layer Wavefront Sensor
NGS	Natural Guide Star
SE	Star Enlarger
PR-I	Pupil Re-Imager

4 Introduction

The Ground layer Wavefront Sensor (GWS) was completely assembled, aligned and tested in the adaptive optics laboratory of the Astronomical Observatory of Padova.

This document includes the Alignment and Verification procedures description used during the GWS DX system re-alignment and verification performed in Heidelberg after the shipping from Padova, together with the obtained alignment results.

The light collected by one of the two arms of LBT will be partially reflected by the annular mirror, positioned on a intermediate focal plane, which is going to reflect the outer 2'-6' annular FoV to the GWS, where the perturbations introduced by the lower part of the atmosphere will be retrieved. A big flange holds 12 motorized remotely-controlled stages which can position up to 12 Star Enlargers (SE) inside the FoV, in order to select the natural guide stars to be used for the wavefront sensing. Each SE increases the F/# of the light coming from a reference star from 15 to 187.5 (it consists of two lens doublets with focal lengths $f1$=13mm and $f2$=162.5mm) and focus it on the pin of a refractive pyramid, which produces four outcoming beams with an angular separation β=0º.566. After this, the Pupil Re-Imager (PR-I), a folded camera composed by a flat folding mirror, a parabolic mirror and a 6-lenses corrector, collects all the beams coming from the SEs and completely superimposes them producing four common images of the entrance pupil of the telescope on the CCD. The PR-I focal length f is 226.8mm.

The distribution of the light between the pupils will allow the reconstruction of the incoming wavefront, according to the Pyramid WFS concept. The detector is mounted on a remotely controllable linear stage for focusing. The whole unit is mounted on a rotation unit to follow the sky. Essentially, it is a big bearing with the purpose to mechanically rotate the complete GWS in order to compensate for the field rotation. This unit consists also of a mount, which connects the GWS to the bench. The GWS mount and rotation unit consist of a cylinder-like case, a bearing system and a support structure.

The bearing is connected to the support structure that links the GWS to the bench on one side and to the cylinder on the other. A motor already integrated with the bearing, moving the whole cylinder-like case, allows following the circular path of the stars within the FoV.

5 Test Equipment

To align the SE to the GWS mechanics, the setup is shown in Fig. 1 has been realized. The idea is to use a wide collimated laser beam, coming from a commercial Fisba interferometer, as a reference, aligned to the GWS so as to be parallel to the GWS optical and rotation axis (coincident after the PR-I alignment).

- The 150 mm wide beam produced with a commercial Fisba interferometer is used as a reference, aligned to the GWS so as to be parallel to the GWS optical and rotation axis.
- A commercial f = 700 mm, 2 inches lens is used to focus part of the wide beam onto the nominal focal plane, defined by the mechanics of the GWS itself.
- A physical stop positioned at the proper distance from the focusing lens (accordingly to the entrance pupil position at LBT: 14 m) defines an F/15 beam.

The focused beam (the green beam in Fig. 1), once passed through a SE, produces four images of the pupil stop on the test CCD. The part of the beam which is not focused by the lens reaches the GWS optics still collimated (the red beams in Fig. 1). If such collimated beam passes through a SE, on the test CCD 4 spots will be produced, whose barycenters are defining the positions of the 4 pupils re-imaged when the same SE is reached by a the beam focused on its entrance focal plane. The part of the collimated beam entering the GWS where no SEs are present focuses on the center of the PR-I FoV.

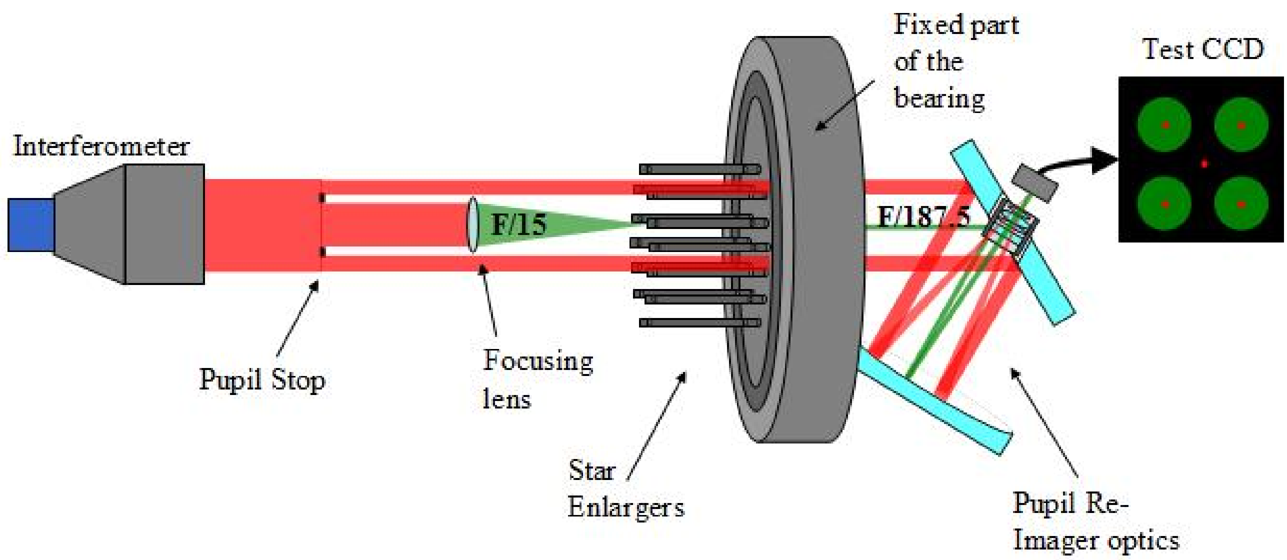

Fig. 1 A wide collimated beam, materializing the GWS rotation axis, is used to align the SEs to the GWS mechanics. Part of such beam is focused onto the nominal mechanical focal plane, producing an F/15 beam which will be used to focus the SEs, looking at the four pupils re-imaged on the test CCD (green beam). The beams which enter the GWS still collimated will produce a spot centered on the center of the field. When such beam goes through the SE, 4 spots are produced on the test CCD, that will be used to align the rotation angle of the pyramid and the SE tip-tilt (red beam).

Component	Characteristic	Value
Interferometer (Fisba + beam expander)	Beam diameter	150 mm
	Beam collimation	Better than 1 arcsec
	Wavelength	633 nm
Pupil stop	Diameter	46.6 mm
	Distance from the lens FP	33.0 mm

Focusing lens	Focal length	700 mm
	Resulting F/#	F/15

Table 1 SE alignment inside GWS setup components main parameters.

6 Verification of Star Enlargers alignment (wrt the rest of GWS) (RS-004-0003)

The star enlarger alignment with respect to the rest of GWS is described in AD3, accordingly to the goal discussed in the GWS Error Budget and reported in Table 2.

Item	Measured Effect	Goal max value	Effect on Error Budget
Pyramid rotation	Four spots rotation	10 arcmin	1/10 sub-aperture
SE tip-tilt	Four spots shift with respect to goal position	9.6 micron	1/5 sub-aperture
SE defocus	Defocus signal	20 nm WFE	/

Table 2 SE alignment procedure goals

Being this the Pathfinder configuration, the SEs have been focused on two different levels (shown in Fig. 2), at a relative distance along the optical axis of 2.57mm. Because of this choice, the SEs operative areas, in this pathfinder configuration, are reduced, as shown in Fig. 3. The residual maximum defocus with respect to the LBT focal surface is 1.37mm.

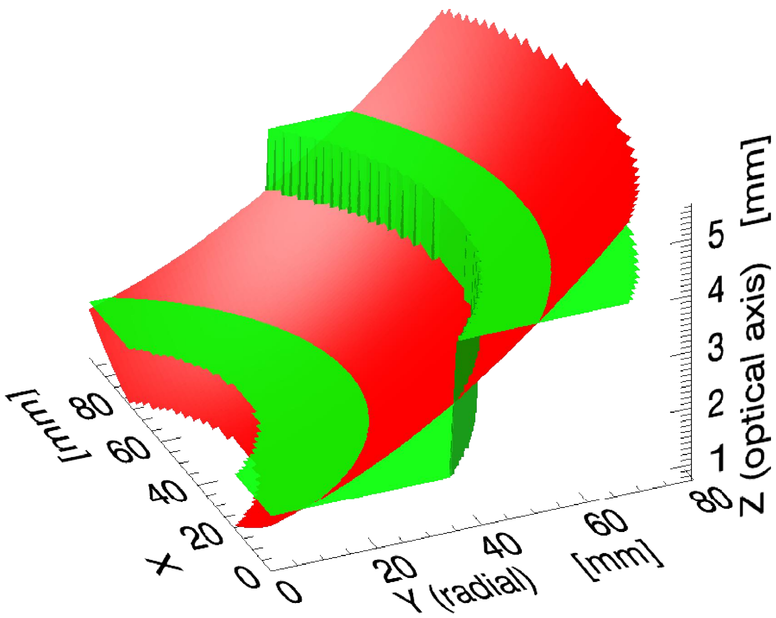

Fig. 2 *Red*: LBT delivered focal surface. *Green*: focus planes in which the SEs are focused in **the Pathfinder mode**. Odd-labeled SEs have been focused to the LBT F/15 beam at a radius R_1 = 62.7mm, while even-labeled SEs have been focused to the LBT F/15 beam at a radius R_2 = 95.7mm. The relative distance of the two planes is 2.57mm.

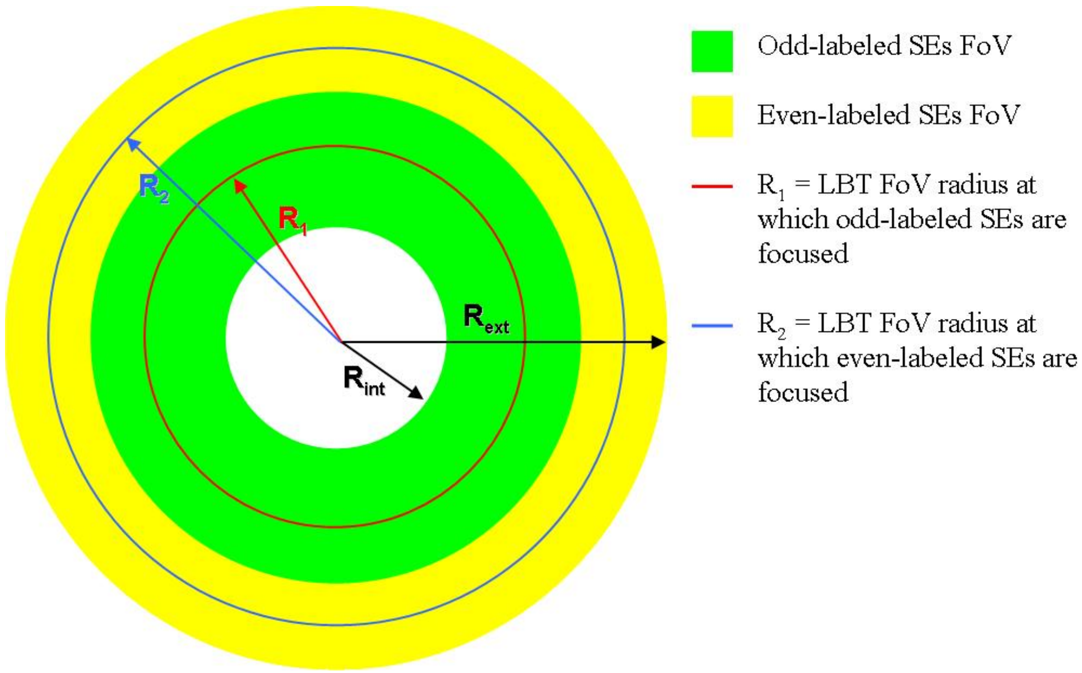

Fig. 3 GWS entrance FoV areas in which the SEs are expected to move in **the Pathfinder mode**. Odd-labeled SEs have been focused to the LBT F/15 beam at a radius R_1 = 62.7mm and are going to move only in the green area (corresponding to a 2.2 arcmin maximum radius). Even-labeled SEs have been focused to the LBT F/15 beam at a radius R_2 = 95.7mm and are going to move only in the yellow area.

Also the SEs alignment in tip-tilt has been reached in their mid-range position along the Y axis, that is to say at a radius R_1 for the odd-labeled SEs and R_2 for the even-labeled SEs.

Table 3 summarizes the main results after the star enlargers re-alignment inside the GWS DX.

SE ID	SE tip-tilt [micron]	Pyramid rotation [arcmin]	SE defocus [nm WFE]
SE01	2.1	-5.0	-19.0
SE02	4.5	8.0	-3.3
SE03	1.3	2.1	-7.6
SE04	0.7	6.7	-9.6
SE05	1.7	-3.3	4.1
SE06	1.8	-1.3	5.7
SE07	1.1	2.5	-4.8
SE08	0.5	1.9	10.4
SE09	2.3	-2.4	13.9
SE10	2.1	-5.8	-6.2
SE11	2.0	1.0	4.4
SE12	2.0	-4.6	-6.1

Table 3 SE alignment with respect to the overall GWS results.

Comparing the measured values with the requirements listed in Table 2, the alignment result inside tolerances for all the considered items. In particular, the relative focus requirement is fulfilled without re-focusing the SEs.

7 Verification of Pupil Blur for GWS system rotation

Concerning the issue, described in AD2, about the pupil blur introduced during the GWS system rotation, a verification test has been performed after the SEs alignment to the rest of the GWS system.

The aim of this verification is to measure the RMS blur, measured as the RMS **DIFFERENTIAL** shift of the spots produced by the 12 SEs in the configuration shown in Fig. 1, *red* beam. The goal is to find an RMS shift of the spots, representing the centers of the pupils, compatible with what expected considering the following blur sources (discussed and included in the overall error budget):

- Pyramid vertex angle;
- Pyramid faces orthogonality;
- SE relative tilt;
- Pyramid orientation;
- PRI optical quality (a small fraction, here neglected);
- SE tilt due to support flexures (a fraction. Here considered 1/sqrt(2));
- SE tilt due to ring flexures (a fraction. Here considered 1/sqrt(2));
- SE tilt due to stage flexures (a fraction. Here considered 1/sqrt(2)).

As discussed in AD2, the root sum square of the listed items is 10.5 μm.

After the SEs alignment, the bearing has been rotated and graphs showing the relative movements of the SEs spots for a 60 degrees rotation have been produced.

Because of the expanded Fisba beam diameter (150mm), the odd-labeled SEs could be positioned exactly in the positions inside the FoV used during the alignment, while the even-labeled SEs had to be disposed in a smaller radius (23.1mm closer to the center), in order to be illuminated by the collimated beam.

Fig. 4 shows the resulting spots shifts for all the SEs, whose RMS value is 14.3 μm, which is larger than what we would expect.

However, we have to remember that only the odd-labeled SEs performance are measured in the proper position, while it’s clear that the spots produced by the even-labeled SEs are slightly shifted with respect to the median position of the spots, and that's due to the fact that the wobble of the stages and the pupil re-imager optical quality are playing a role (they should not, in this verification test. In fact they’re not part of the listed blur sources), since the SEs are not exactly in the positions in which they have been aligned.

Fig. 5 shows the results obtained only with the odd-labeled SEs in the field. The RMS relative shift turns to 9.4 microns (below the expectations), and we have no reason to expect something different from the even-labeled SEs, if they’re performance would be verified in the proper field positions, since they've been aligned with the same precision than the odd-labeled ones.

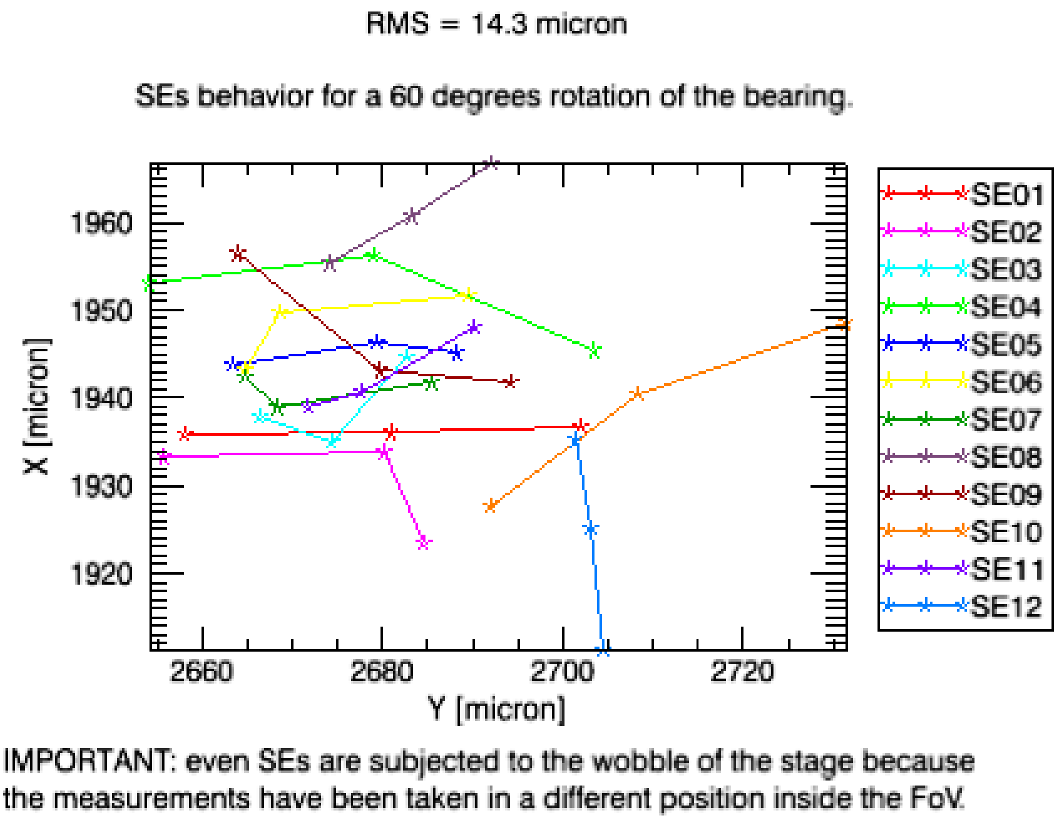

Fig. 4 all the SEs together in the field. The RMS relative shift is 14.3 microns, but it's clear that the spots produced by the even-labeled SEs are slightly shifted with respect to the median position of the spots, since the SEs are not exactly in the positions in which they have been aligned.

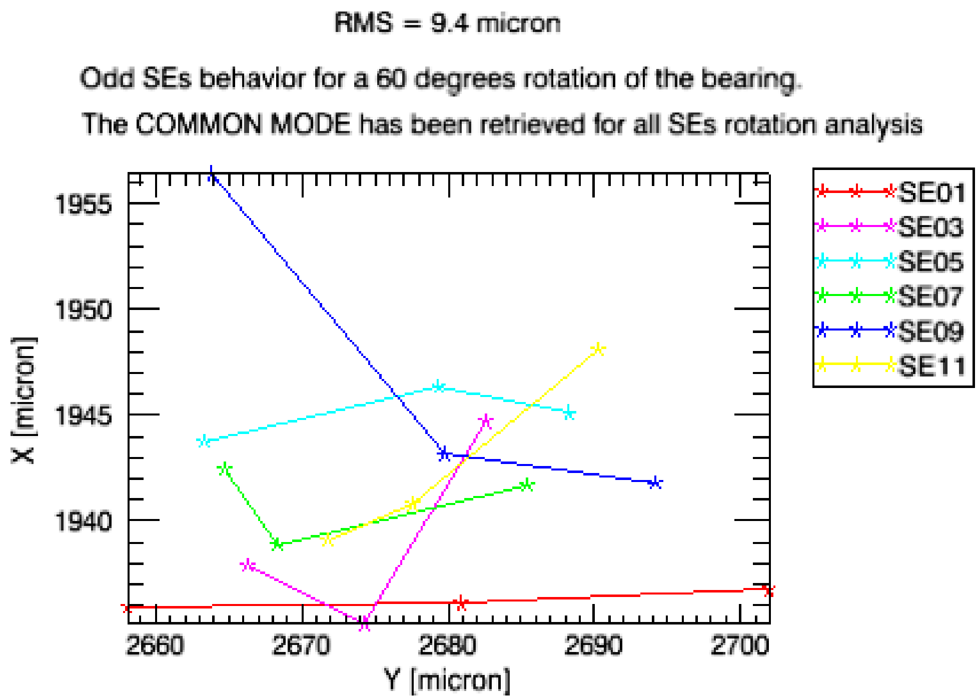

Fig. 5 only the odd-labeled SEs, same curves as the previous graph.